



AIAA 96-1677

**A Study of Wave Propagation in a Duct
and Mode Radiation**

F. Farassat

NASA Langley Research Center
Hampton, VA

M. K. Myers

The George Washington University
Hampton, VA

2nd AIAA/CEAS Aeroacoustics Conference
May 6-8, 1996/State College, PA

A STUDY OF WAVE PROPAGATION IN A DUCT AND MODE RADIATION

F. Farassat*

Fluid Mechanics and Acoustics Division
NASA Langley Research Center
Hampton, Virginia

M. K. Myers**

The George Washington University
Joint Institute for Advancement of Flight Sciences
NASA Langley Research Center
Hampton, Virginia

Abstract

In this paper we discuss two problems of classical duct acoustics: (1) wave propagation in infinite ducts with uniform flow based on a graphical approach, and (2) detection of mode radiation from a duct by an external circular microphone array. In (1) we show that the wave number vectors for a given flow Mach number form an ellipse whose center and shape depend on the Mach number only. We construct graphically the upstream and downstream wave number vectors of modes that propagate in the duct. We then show how one can infer from this graphical approach many known results in duct propagation such as the mode cut-off concept, the direction of energy propagation, the angle of the radiation lobe at peak directivity using Rice's cut-off ratio concept, and other qualitative results. In (2) we give the mathematics behind the experimental detection of mode radiation from a duct by a circular array of microphones whose axis coincides with the engine axis. Since the external microphone array does not introduce additional noise sources inside the engine, as does a rotating rake of microphones positioned at the inlet, this measurement technique may be preferable to use of a rotating rake. The simplicity afforded by the lack of sophisticated rotating parts is an additional advantage over the rotating array.

Introduction

Acoustic wave propagation through a flow in an infinite duct and sound radiation from a duct inlet are

old problems of acoustics. Both are relevant to the design and understanding of the noise characteristics of ducted fan engines. Noise is generated inside the engine by various flow related mechanisms, e.g., rotor wake-stator interaction, and then propagates through the inlet and exhaust ducts. Although the duct length in all engines is finite in length, the study of acoustic wave propagation in infinite ducts of circular or annular shapes has been very useful to engine designers both qualitatively and quantitatively. The basic paper on infinite duct acoustic wave propagation is by Tyler and Sofrin¹. There are many useful results in this paper and elsewhere on infinite duct propagation that one should understand in order to explain some aspects of engine noise. A real engine, however, has nonuniform flow within the duct which complicates the problem of acoustic wave propagation considerably^{2,3}. One would then like to know what modes are generated inside and propagated out of the inlet and the exhaust. One way of finding modes that escape out of the duct is by using a rotating microphone array⁴. However, the rotating microphone array produces a wake that may interact with a fan rotor and produce additional noise. It would be preferable if one could use a noninvasive experimental method of detecting escaping modes in place of a rotating microphone array.

In this paper we intend to present two results related to the acoustic problems discussed in the above paragraph. First, we give a graphical representation of wave propagation in an infinite duct carrying a uniformly moving fluid. We show that many known results can be derived easily by this graphical method. The method relies on construction of an ellipse in wave number space whose shape is dependent on flow speed. The propagating waves as well as upstream and

*Senior Research Scientist, Associate Fellow AIAA.

**Professor, Associate Fellow AIAA.

downstream wave number vectors are then constructed graphically. The direction of energy propagation, the mode cut-off concept and the approximate radiation angle for each mode can all be constructed graphically also. Second, we propose a new method for experimental detection of modes escaping from a finite duct using an external circular array of microphones whose axis coincides with the engine axis. We give the theory behind mode detection here. Such an array has been constructed at Langley Research Center and will soon be tested in an anechoic room using a model ducted fan engine.

Graphical Approach to Wave Propagation in a Uniform Duct With Flow

Consider a duct of uniform circular or annular cross section carrying a uniform flow at Mach number $M < 1$. The differential equation and the boundary condition for propagation of small pressure perturbations for the hard wall case is

$$\begin{cases} \left(\frac{1}{c_0} \frac{\partial}{\partial t} + M \frac{\partial}{\partial x} \right)^2 p' - \nabla^2 p' = 0 & (1-a) \\ \frac{\partial p'}{\partial r} = 0 \quad (\text{on the wall}) & (1-b) \end{cases}$$

in which x is the axial coordinate along the duct. If cylindrical polar coordinates (r, θ, x) are used, and if it is assumed that a complex solution for the acoustic pressure p' exists in the form

$$p' = P(r, \theta, x) e^{i\omega t} \quad (2)$$

then the complex amplitude P satisfies the equations

$$\begin{cases} (1 - M^2) \frac{\partial^2 P}{\partial x^2} + \nabla_2^2 P - 2ikM \frac{\partial P}{\partial x} + k^2 P = 0 & (3-a) \\ \frac{\partial P}{\partial r} = 0 \quad (\text{on the wall}) & (3-b) \end{cases}$$

in which $k = \omega/c_0$ and ∇_2^2 is the two-dimensional Laplacian in polar coordinates.

Let $k_x(m, n)$ and $k_r(m, n)$ be the axial and radial wave numbers for the m th circumferential and n th radial modes. Considering a circular duct of radius R now, the solution of Eq. (1) for the mode (m, n) is

$$p' = A_{mn} J_m[k_r(m, n)r] \exp i[\omega t - m\theta - k_x(m, n)x] \quad (4)$$

where the $k_r(m, n)$ are obtained as the roots of

$$J'_m[k_r(m, n)R] = 0 \quad (5)$$

numbered in consecutive order by $n=1, 2, 3, \dots$. Here $J_m(\cdot)$ is the Bessel function of the first kind of order m . Let $\beta^2 = 1 - M^2$. Then $k_x(m, n)$ is given from Eqs. (3) and (4) by

$$\begin{aligned} k_x(m, n) &= \frac{k}{\beta^2} \left[-M \pm \sqrt{1 - [\beta k_r(m, n)/k]^2} \right] \\ &= \frac{k}{\beta^2} \left[-M \pm \sqrt{1 - 1/\beta_{mn}^2} \right] \end{aligned} \quad (6)$$

in which $m=0, 1, 2, \dots$. We have defined the cut-off ratio β_{mn} as

$$\beta_{mn} = \frac{k}{\beta k_r(m, n)} \quad (7)$$

It then follows that the mode (m, n) is propagating if $\beta_{mn} > 1$ and decaying if $\beta_{mn} < 1$.

In preparation for the graphical approach, we write Eq. (6) as follows

$$\frac{(\tilde{k}_1 + M/\beta^2)^2}{1/\beta^4} + \frac{\tilde{k}_2^2}{1/\beta^2} = 1 \quad (8)$$

where $\tilde{k}_1 = k_x/k$ and $\tilde{k}_2 = k_r/k$. For use later we note that Eq. (8) can also be expressed as

$$\tilde{k}_1^2 + \tilde{k}_2^2 = (1 - M\tilde{k}_1)^2 \quad (9)$$

Equation (8) is an ellipse in the variables $(\tilde{k}_1, \tilde{k}_2)$ with center at $(-M/\beta^2, 0)$ and with semi-major and semi-minor axes $1/\beta^2$ and $1/\beta$, respectively. The ellipse depends only on M . It intersects the \tilde{k}_1 axis at $\tilde{k}_1 = 1/(1+M) > 0$ and $\tilde{k}_1 = -1/(1-M) < 0$. It always intersects the \tilde{k}_2 axis at $\tilde{k}_2 = \pm 1$. Figure 1 shows the ellipse described by Eq. (8) for flow Mach number $M=0.8$. Note that for $M=0$, Eq. (8) gives a circle of

unit radius in the $\tilde{k}_1\tilde{k}_2$ plane with its center at the origin. We now use this ellipse to study some aspects of wave propagation in a circular duct.

i) Propagating and Decaying Modes: Figure 2 shows how one determines the propagating and decaying modes. On different vertical axes, each corresponding to a circumferential mode m , plot the solutions of Eq. (5), i.e. $k_r(m,n)/k$ for $n=1,2,\dots$. Draw horizontal lines as shown in this figure for $m=0$. If these lines intersect the ellipse, the mode (m,n) is a propagating mode. Otherwise the mode is decaying. In general, we get two values for k_a which we denote as k_{a+} and k_{a-} . In Fig. 2 we have shown $k_{a+}(0,3)/k$ and $k_{a-}(0,3)/k$. Note that k_a determines the axial phase speed of the mode (m,n) . The k_{a+} mode is generally called the downstream mode, but any propagating k_{a+} mode for which $k_r/k > 1$ actually moves in the negative x direction; this is the case with $k_{a+}(0,3)$ on Fig. (2). The relationship of the phase speed of the mode to the velocity of energy propagation in the mode will be discussed below.

ii) Mode Cut-off and Energy Flow: When the cut-off ratio β_{mn} is equal to unity, $\tilde{k}_2 = 1/\beta$. Since the semi-minor axis of the ellipse in the $\tilde{k}_1\tilde{k}_2$ plane is $1/\beta$, the axial wave number corresponding to $\tilde{k}_2 = 1/\beta$ is $\tilde{k}_1 = k_a/k = -M/\beta^2$. Figure 3 shows the wave number vector for the cut-off condition at $M=0.8$. It indicates that the k_{a+} wave propagates upstream. To discover what is special about the wave number vector at cut-off we consider the acoustic energy flux vector for the modal solution given by Eq. (4).

For isentropic disturbances in a uniform flow at velocity \tilde{V} the acoustic energy flux vector can be written as⁵

$$\begin{aligned}\tilde{W} &= (p' + \rho_0 \tilde{V} \cdot \tilde{u}') \left(\tilde{u}' + \frac{p'}{\rho_0 c_0^2} \tilde{V} \right) \\ &= (p' + \rho_0 c_0 \tilde{M} \cdot \tilde{u}') \left(\tilde{u}' + \frac{p'}{\rho_0 c_0} \tilde{M} \right)\end{aligned}\quad (10)$$

In Eq. (10), \tilde{u}' is the acoustic particle velocity corresponding to p' , ρ_0 is the density of the undisturbed flow, and \tilde{M} is the flow Mach number vector \tilde{V}/c_0 . The (primed) disturbance quantities are the actual (real) acoustic pressure and velocity. For an acoustic field represented in the complex form of Eq. (4) the linearized equation of linear momentum gives

$$\tilde{u}' = \frac{-\nabla p'}{i \rho_0 c_0 k (1 - M \tilde{k}_1)} = \frac{\tilde{k}_1 p'}{\rho_0 c_0 (1 - M \tilde{k}_1)} \tilde{e}_1 + \tilde{u}'_2 \quad (11)$$

in which \tilde{e}_1 is the unit vector along x and \tilde{u}'_2 is the projection of \tilde{u}' on the cross-sectional plane of the duct. Thus, for the single-mode complex solution given by Eq. (4) we have

$$\tilde{W} = \text{Re} \left[\frac{p'}{1 - M \tilde{k}_1} \right] \cdot \text{Re} \left[\frac{\beta^2 \tilde{k}_1 + M}{\rho_0 c_0 (1 - M \tilde{k}_1)} p' \tilde{e}_1 + \tilde{u}'_2 \right] \quad (12)$$

Here $\text{Re}[\cdot]$ denotes the real part of $[\cdot]$. We see from Eq. (12) that at the cut-off condition, $\tilde{k}_1 = -M/\beta^2$, the axial component of the acoustic energy flux vanishes: \tilde{W} is normal to the wall and no energy propagates along the duct axis.

This cut-off of axial energy flux can also be exhibited graphically on the wave number ellipse, although only approximately for a circular duct (the interpretation is exact for ducts of rectangular cross-section). For this purpose we use the large argument approximation of the Bessel function

$$J_m(k_r r) \approx \sqrt{\frac{2}{\pi k_r r}} \cos(k_r r - \psi_m) \quad (13)$$

with $\psi_m = \pi/4 + m\pi/2$ to approximate p' by

$$\begin{aligned}p' &\approx \frac{A_{mn}}{2} \sqrt{\frac{2}{\pi k_r r}} \{ \exp i[\omega t - m\theta - k_a x - k_r r - \psi_m] + \\ &\quad \exp i[\omega t - m\theta - k_a x + k_r r + \psi_m] \}\end{aligned}\quad (14)$$

We see that, for sufficiently large k_r at any fixed θ , p' can be considered to be the sum of two progressing waves in (x, r) whose phases are

$$\phi_{\pm} = \omega t - k_a x \mp k_r r = k(c_0 t - \tilde{k}_1 x \mp \tilde{k}_2 r) \quad (15)$$

The unit vectors normal to these planar phase surfaces are $\tilde{n}_{\pm} = -\nabla \phi_{\pm} / |\nabla \phi_{\pm}|$, or

$$\tilde{n}_{\pm} = \frac{(\tilde{k}_1, \pm \tilde{k}_2)}{\sqrt{\tilde{k}_1^2 + \tilde{k}_2^2}} = \frac{(\tilde{k}_1, \pm \tilde{k}_2)}{1 - M \tilde{k}_1} \quad (16)$$

where we have used Eq. (9). Now if we invert Eq. (16) to express the wave number vector $\vec{k}_x = (\bar{k}_1, \pm \bar{k}_2)$ in terms of \vec{n}_x , we obtain

$$\vec{k}_x = \vec{n}_x / (1 + \vec{M} \cdot \vec{n}_x) \quad (17)$$

If we use Eq. (17) in Eq. (15) we find

$$\phi_x = \omega t - \frac{k \vec{n}_x \cdot \vec{r}}{1 + \vec{M} \cdot \vec{n}_x} \quad (18)$$

where \vec{r} is the position vector (x,r) in the plane of constant θ . The phases in Eq. (18) are precisely those of a pure plane wave propagating in the directions \vec{n}_x in the (x,r) plane. The phase speeds of these waves are, from Eq. (18), $c_0(1 + \vec{M} \cdot \vec{n}_x)$.

If the approximation is viewed locally and variations in the geometric factor $r^{-1/2}$ are ignored, then Eq. (14) implies that at points sufficiently close to the duct wall at least the higher order n modes can be interpreted as being a sum of two interfering plane waves propagating in the directions \vec{n}_x . For each of these separately the relation $\bar{u}' = p' / \rho_0 c_0$ holds so that the energy flux associated with each is given from Eq. (10) by

$$\bar{W} = \frac{p'^2}{\rho_0 c_0^2} (1 + \vec{M} \cdot \vec{n}) (c_0 \vec{n} + \vec{V}) \quad (19)$$

The last factor in Eq. (19) is the energy propagation velocity, or the group velocity \vec{V}_G , of the plane wave:

$$\vec{V}_G = c_0 \vec{n} + \vec{V} = c_0 (\vec{n} + \vec{M}) \quad (20)$$

and it is this quantity associated with the approximate plane wave representation of the duct modes that is convenient to consider in conjunction with the wave number ellipse.

If we again refer to Fig. (3), we see that at cut-off the component of \vec{V}_G in the x direction is

$$\vec{V}_G \cdot \vec{e}_1 = c_0 (-\cos \theta_c + M) = c_0 (-M + M) = 0 \quad (21)$$

Here we have used the fact that, as seen from Fig. 3, $\tan \theta_c = \beta/M$ and thus $\cos \theta_c = M$, where θ_c is the angle that \vec{k} at the cut-off condition makes with the \vec{k}_1 -axis. Equation (21) means that the acoustic energy flux vector is normal to the wall and no energy is propagated along the axis.

To find the direction of group velocity in our graphical construction follow the vector diagram of Fig. 4. This diagram is in the $\vec{k}_1 \vec{k}_2$ plane so that \vec{M} must be scaled up to \vec{M}/β^2 to get the direction of the group velocity as shown in this plane. From the figure, it is clear that at the cut-off condition the group velocity points upward, and thus the energy flux vector is normal to the wall.

iii) The Angle Of The Main Lobe Of Radiation From An Inlet: Rice, Heidmann and Sofrin⁶ have proposed a rule for finding the angle of the main lobe of radiation from an inlet where the duct Mach number is M and the inflow Mach number (flight speed) is M_∞ . By our graphical method we can give a simple interpretation of their rule as follows. Intuitively, it is obvious that the phase velocity of a radiating mode at the inlet should be based on M, the duct flow Mach number. But the angle of the main lobe of radiation is in the direction of the group velocity using \vec{M}_∞ instead of \vec{M} in Fig. 4. Figure 5 shows this construction. Here θ' is the sought angle. The mathematical reasoning is as follows. Remembering that $\bar{k}_1 < 0$, we have, from Fig. 5:

$$\tan \theta' = \frac{\bar{k}_2}{\bar{k}_1 + M_\infty / \beta^2} = \frac{\beta}{|(M_\infty - M) \beta_{mn} - \sqrt{\beta_{mn}^2 - 1}|} \quad (22)$$

where β_{mn} is the cut-off ratio. This is equivalent to the expression that Rice, et.al.⁶, gave for $\cos \theta'$.

iv) Other Results: One can easily show graphically some other known results. One is the following: if a mode (m,n) propagates for $M=M_1$, then it will propagate for duct Mach number $M_2 > M_1$. The proof is simple. From Fig. 6 the semi-minor axis of the ellipse for M_2 is

$1/\beta_2$, where $\beta_2 = \sqrt{1 - M_2^2} < \beta_1 = \sqrt{1 - M_1^2}$. Therefore, $1/\beta_2 > 1/\beta_1$ = semi-minor axis of the ellipse for M_1 . Hence, a horizontal line that intersects the ellipse for $M=M_1$ necessarily intersects the ellipse for $M=M_2$. See Fig. (6).

Another result is that as $M \rightarrow 1$ all modes will propagate. Again the graphical proof is very simple. As $M \rightarrow 1$, $\beta \rightarrow 0$ and the equation of the ellipse degenerates into the parabola

$$\tilde{k}_2^2 = 1 - 2\tilde{k}_1 \quad (23)$$

The axis of this parabola is the \tilde{k}_1 -axis and the parabola intersects the \tilde{k}_1 -axis at $\tilde{k}_1 = 1/2$. The parabola extends to infinity in the \tilde{k}_2 direction so that any horizontal line intersects it. See Fig. 7. This means, by our graphical method of discovering propagating modes, that all modes propagate.

We mention here that the ellipse of Fig. 1 remains unchanged for 2-dimensional, 3-dimensional rectangular, and annular ducts. Only the values of \tilde{k}_2 for the modes, which depend on the duct geometry, will change.

Detection of Mode Radiation From a Duct by an External Microphone Array

In this section we describe the mathematics of mode detection by use of a circular microphone array. The axis of this array coincides with engine axis. We consider a static engine here ($M=0$). We assume that we can approximate the radiation from the inlet by the Rayleigh formula

$$4\pi p'(\vec{x}, t) = \frac{\partial}{\partial t} \int_{\text{inlet}} \frac{[\rho_0 u]_{\text{ret}}}{\tilde{R}} dS \quad (24)$$

where U is the axial acoustic particle velocity at the inlet, and \tilde{R} is the radiation distance from points in the inlet plane. We will concentrate on a frequency of $\alpha \times \text{BPF} = \alpha B\Omega$, where B is the number of fan blades and Ω is the angular velocity of the fan. Let us assume that we have V vanes, or a circumferentially periodic disturbance of period $2\pi/V$ radians. We know that we generate circumferential modes $m = \alpha B + qV$ where $q = \pm 1, \pm 2, \dots$. Let n be the radial mode number index of the acoustic waves that propagate and radiate out of the inlet. The acoustic pressure in the duct for frequency $\alpha B\Omega$ is

$$p' = \exp i[\alpha B(\Omega t - \theta)] \sum_n \sum_q A_{nq} J_m[k_r(m, n)r] \times \exp\{-i[qV\theta + k_a(m, n)x]\} \quad (25)$$

Note that m is a function of q in Eq. (25).

The relation between u and p' for frequency $\alpha B\Omega$ is:

$$u = \frac{1}{\alpha B\Omega \rho_0} \exp i[\alpha B(\Omega t - \theta)] \times \sum_n \sum_q A_{nq} k_a(m, n) J_m[k_r(m, n)r] \times \exp\{-i[qV\theta + k_a(m, n)x]\} \quad (26)$$

Now let us assume that the origin of the cylindrical polar coordinates is at $x=0$. Then

$$u(r, \theta, 0) = \frac{1}{\alpha B\Omega \rho_0} \exp i[\alpha B(\Omega t - \theta)] \times \sum_n \sum_q A_{nq} k_a(m, n) J_m[k_r(m, n)r] e^{-iqV\theta} \quad (27)$$

Let a microphone on a circular array of radius a from the x axis have cylindrical polar coordinates (a, θ', x) . From a point on the inlet with coordinates (r, θ) , the radiation distance is

$$R \approx R_0 - r \sin \psi \cos(\theta - \theta') \quad (28)$$

where $R_0 = \sqrt{a^2 + x^2}$ is the distance of the microphone from the center of the inlet and $\sin \psi = a/R_0$, i.e. ψ is the angle that the microphone makes with the engine axis. We are assuming that $r_0/R_0 \ll 1$, where r_0 is the inlet radius.

Using Eq. (27) in Eq. (24), we get

$$\begin{aligned}
4\pi p'(a, \theta', x, t) &= \frac{i\pi}{\rho_0} \exp\left\{i\alpha B\left[\Omega\left(t - \frac{R_0}{c}\right) - \theta'\right]\right\} \sum_n \sum_q A_{nq} k_a(m, n) e^{-iqv\theta'} \int_0^{r_0} \int_0^{2\pi} J_m[k_r(m, n)r] \times \\
&\quad \exp\left\{-\left(\alpha B + qV\right)(\theta - \theta') + \frac{\alpha B \Omega r}{c_0} \cos(\theta - \theta') \sin \psi\right\} r dr d\theta \\
&= \frac{i\pi}{\rho_0} \exp\left\{i\alpha B\left[\Omega\left(t - \frac{R_0}{c}\right) - \theta'\right]\right\} \sum_n \sum_q A_{nq} k_a(m, n) e^{-iqv\theta'} \int_0^{r_0} J_m[k_r(m, n)r] J_m\left[\frac{\alpha B \Omega r}{c_0} \sin \psi\right] r dr \\
&= \frac{i\pi}{\rho_0} D(\theta') \exp\left\{i\alpha B\left[\Omega\left(t - \frac{R_0}{c}\right) - \theta'\right]\right\} \quad (29)
\end{aligned}$$

where $D(\theta')$ is a periodic function of θ' with first harmonic $2\pi/V$.

From Eq. (29), we see that since

$$D(\theta') = \sum_q D_q e^{-iqv\theta'} \quad (30)$$

a complex Fourier transform of $D(\theta')$, which is obtained by microphone measurement, will give all q 's (positive and negative integers) and therefore all circumferential modes for $\alpha \times BPF$. Once all the q 's are found, then we can numerically compute

$$C(m, n, \psi) = \int_0^{r_0} r J_m[k_r(m, n)] J_m\left(\frac{\alpha B \Omega r}{c_0} \sin \psi\right) dr \quad (31)$$

From Eq. (26), for a fixed q , we have

$$D_q = \sum_m k_a(m, n) C(m, n, \psi) A_{nq} \quad (32)$$

Using N positions of the microphone array, we can find N propagating radial modes corresponding to the circumferential mode $m = \alpha B + qV$. We propose to use singular value decomposition in order to invert Eq. (32) to find A_{nq} . Extension to the case of a moving engine is similar and straightforward.

Recently it has come to the authors' attention that B. J. Tester, et. al.⁷, have described a similar method for mode detection based on pressure cross-spectrum versus separation in polar angle. The authors are now studying the possibility that the method of Ref. 7 can be combined with that of the current paper.

References

1. Tyler, J. M. and Sofrin, T. G., "Axial Flow Compressor Noise Studies," *SAE Transactions*, Vol. 70, 1962, p.p. 309-332.
2. Nayfeh, A. H., Kaiser, J. E. and Shaker, B. S., "A Wave-Envelope Analysis of Sound Propagation in Non-uniform Circular Ducts With Compressible Mean Flows," NASA CR-3109, March, 1979.
3. Uenishi, K. and Myers, M. K., "Two-Dimensional Acoustic Field in a Nonuniform Duct Carrying Compressible Flow," *AIAA Journal*, Vol. 22, No. 9, September, 1984, p.p. 1242-1248.
4. Heidelberg, L. J. and Hall, D. G., "Inlet Acoustic Mode Measurements Using a Continuously Rotating Rake," *J Aircraft*, Vol. 32, No. 4, July-August, 1995, p.p. 761-767.
5. Myers, M. K., "An Exact Energy Corollary for Homentropic Flow," *J. Sound and Vibration*, Vol. 109, No. 2, 1986, p.p. 277-284.
6. Rice, E. J., Heidmann, M. F. and Sofrin, T. G., "Modal Propagation Angles in a Cylindrical Duct with Flow and Their Relation to Sound Radiation," AIAA Paper 79-0183, January, 1979.
7. Tester, B. J., Cargill, A. and Barry, B., "Fan Noise Duct-Mode Detection in the Far-Field: Simulation, Measurement and Analysis," AIAA Paper 79-0580, March, 1997.

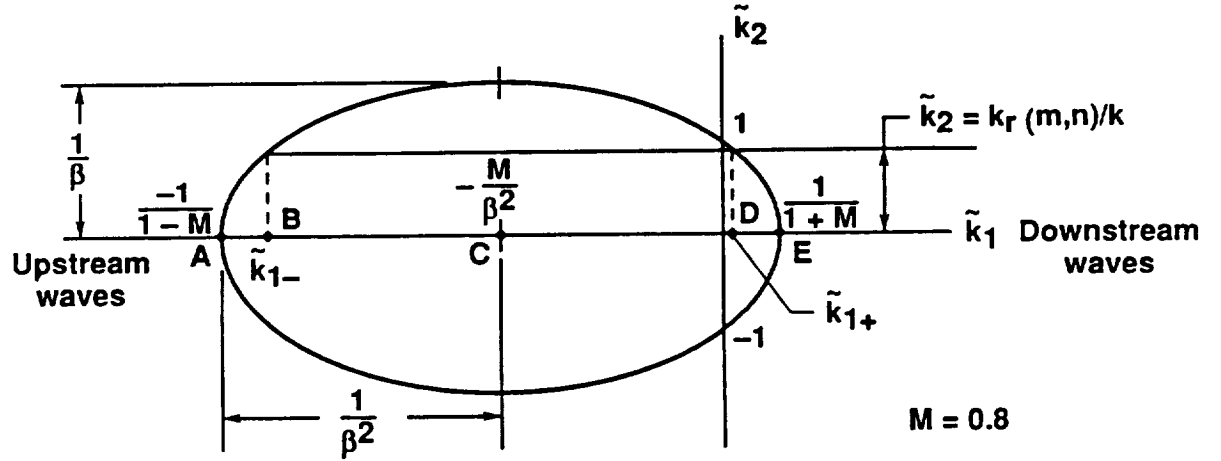


Fig. 1 - The ellipse of wave number vector described by Eq. (8); $\tilde{k}_1 = k_a/k, \tilde{k}_2 = k_r/k$. Corresponding to each propagating wave with a given \tilde{k}_2 , two axial wave numbers \tilde{k}_{1+} and \tilde{k}_{1-} are obtained.

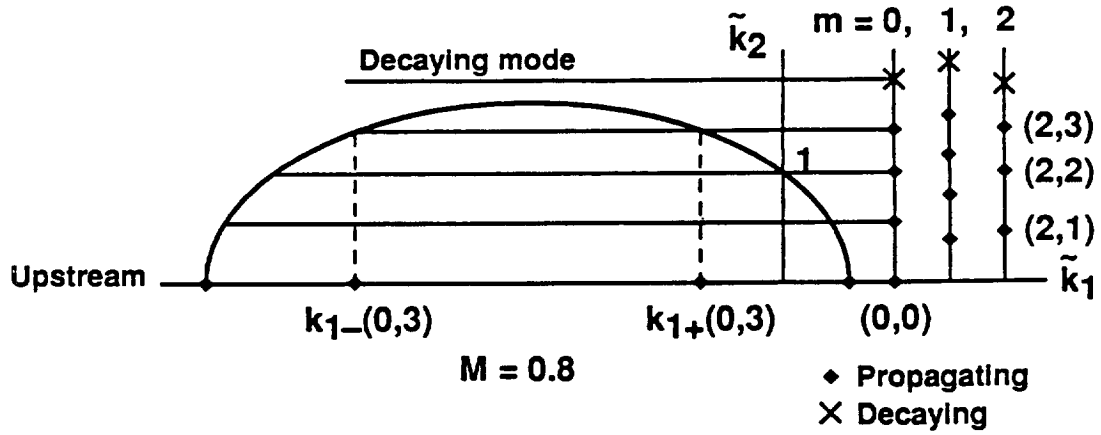


Fig. 2. - Determination of propagating and decaying waves. Each vertical line on the right corresponds to one circumferential mode.

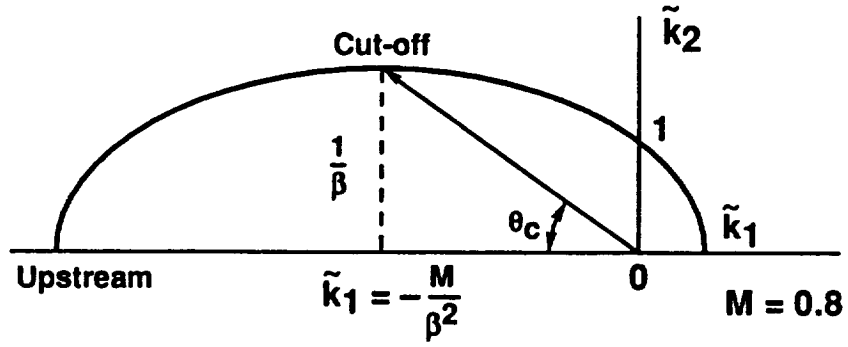


Fig. 3. - The wave number vector at cut-off

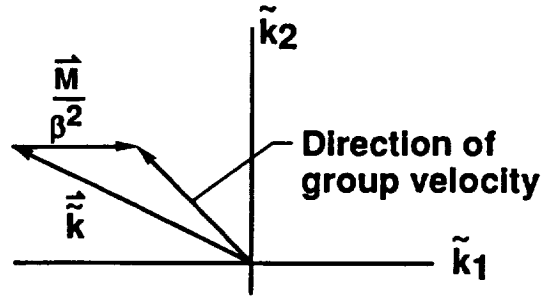


Fig. 4. - The diagram for finding the direction of group velocity in the $\tilde{k}_1 \tilde{k}_2$ -plane.

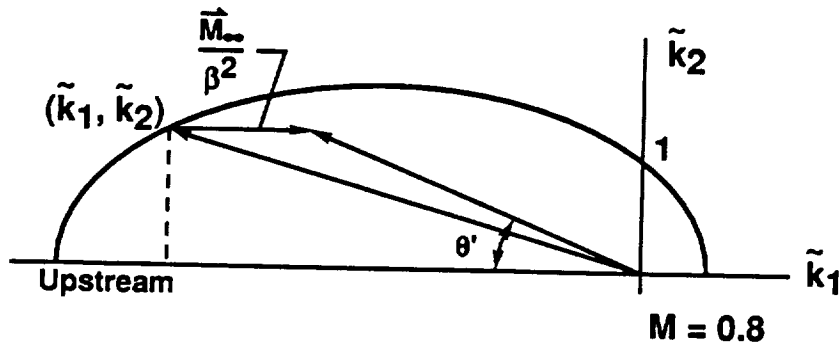


Fig. 5. - The diagram for construction of θ' , the angle of the main radiation lobe from an inlet, as proposed by Rice, Heidmann and Sofrin⁵. The ellipse is based on the duct Mach number and the flight Mach number is M_∞ .

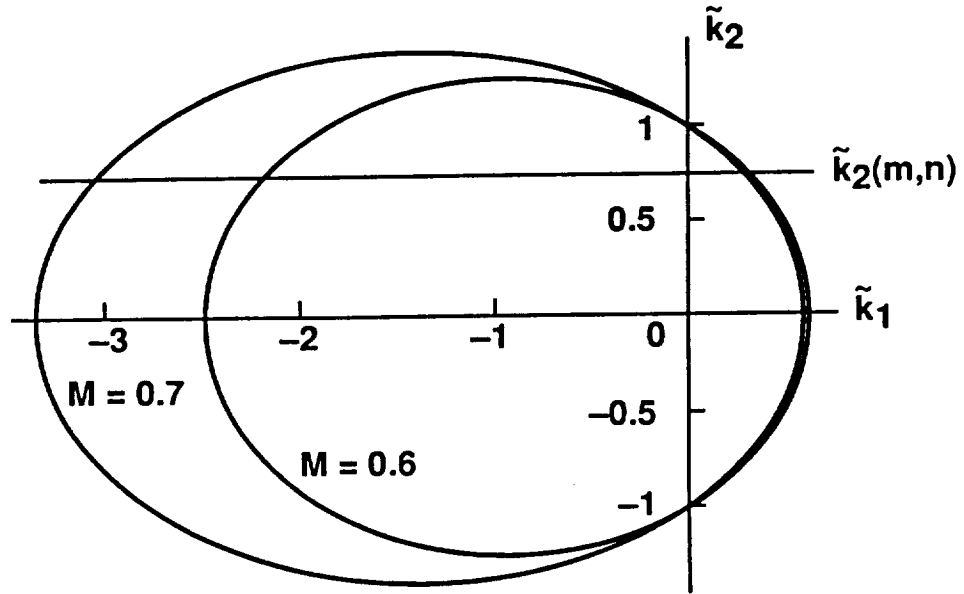


Fig. 6. - The ellipses for $M=0.6$ and $M=0.7$. Mode (m,n) propagates for $M=0.6$. Therefore it propagates for $M>0.6$.

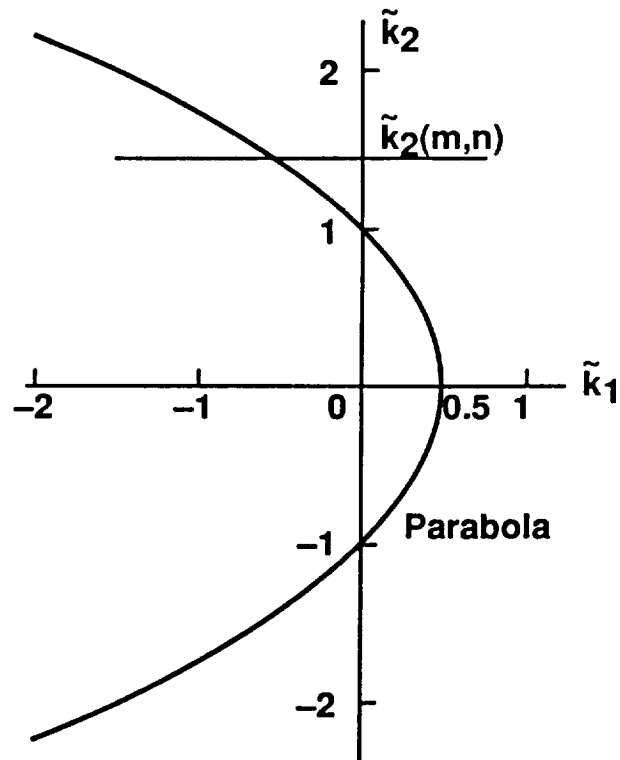


Fig. 7. - The degenerate ellipse (a parabola) as $M \rightarrow 1$. Note that as $\tilde{k}_1 \rightarrow -\infty$, we have $\tilde{k}_2 \rightarrow \pm\infty$. Any horizontal line intersects the parabola, i.e., all modes propagate.

